The effects of Diffusive Shock Acceleration on the Emitted X-ray Spectrum in SNR Shocks

Dan Patnaude
SAO

Don Ellison (NCSU)
Pat Slane (SAO)
Rob Fesen (Dartmouth)
Jacco Vink (Utrecht)
Martin Laming (NRL)

DSA: A Brief Overview

- Efficient diffusive shock acceleration lowers the shock temperature and raises the postshock density (Jones & Ellison, 1991; Berezhko & Ellison, 1999)
- The nonequilibrium ionization is dependent upon both the shock temperature and the shock density through their relation to the electron temperature, T_e, and electron density, n_e
- A number of Galactic SNRs show both thermal and nonthermal emission behind the forward shock, including SN1006 (Vink et al. 2003; Bamba et al. 2008), Tycho (Hwang et al. 2002; Cassam-Chenaï et al. 2007) and Cas A (Araya et al. 2010)
- In SNR RX J 1713.7-3946, the lack of thermal X-ray emission is an important constraint on the ambient density and significantly impacts models for TeV emission (Ellison et al. 2001, Aharonian et al. 2007; Katz & Waxman 2008, Ellison, Patnaude, Slane, & Raymond, 2010)

EVIDENCE FOR EFFICIENT DSA IN SNRS

Efficient shock accleration softens the EOS in the shocked gas. In Tycho, the location of the blastwave suggests that it has been modified considerably by cosmic ray acceleration.

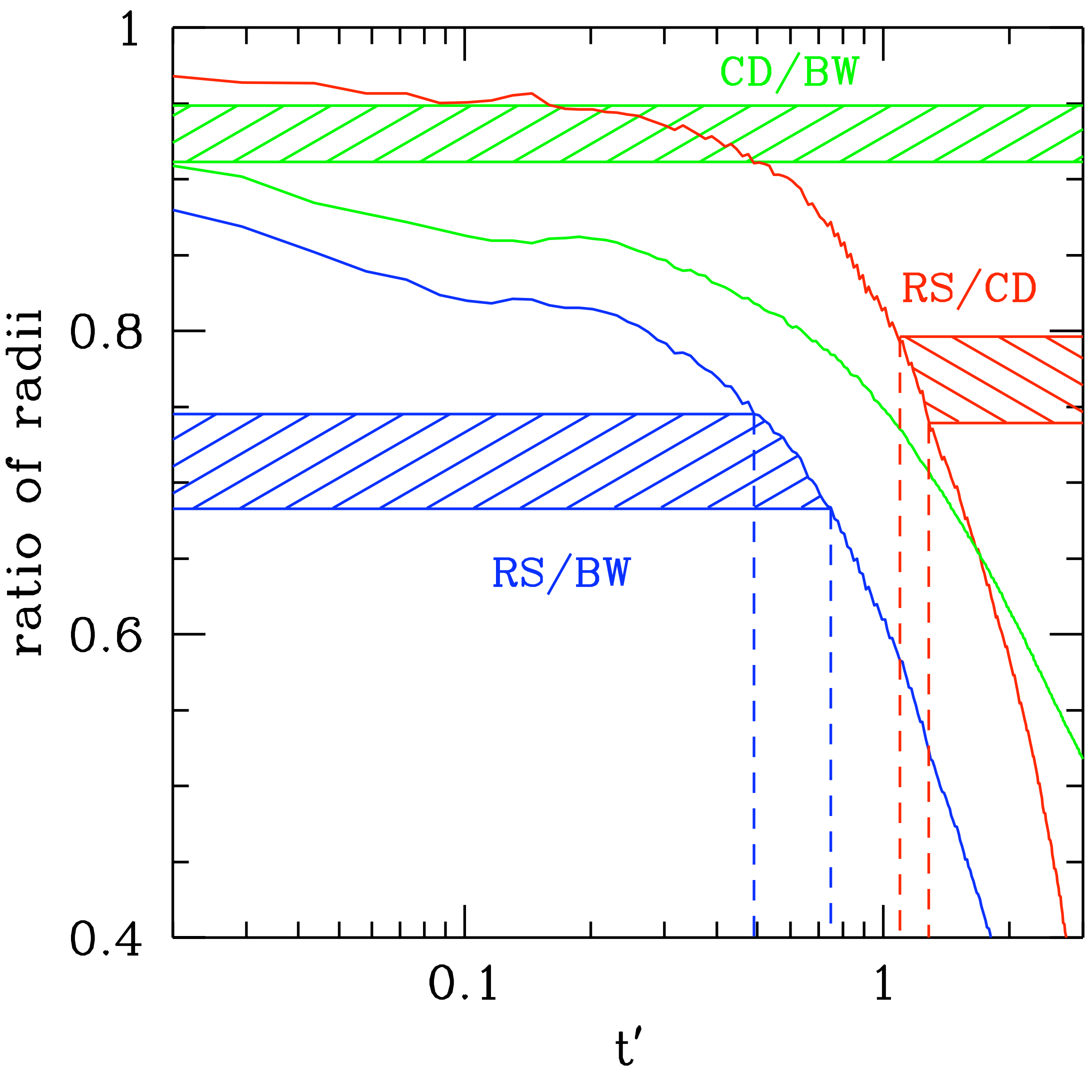

Time evolution of Tycho's SNR (Warren et al. 2005)

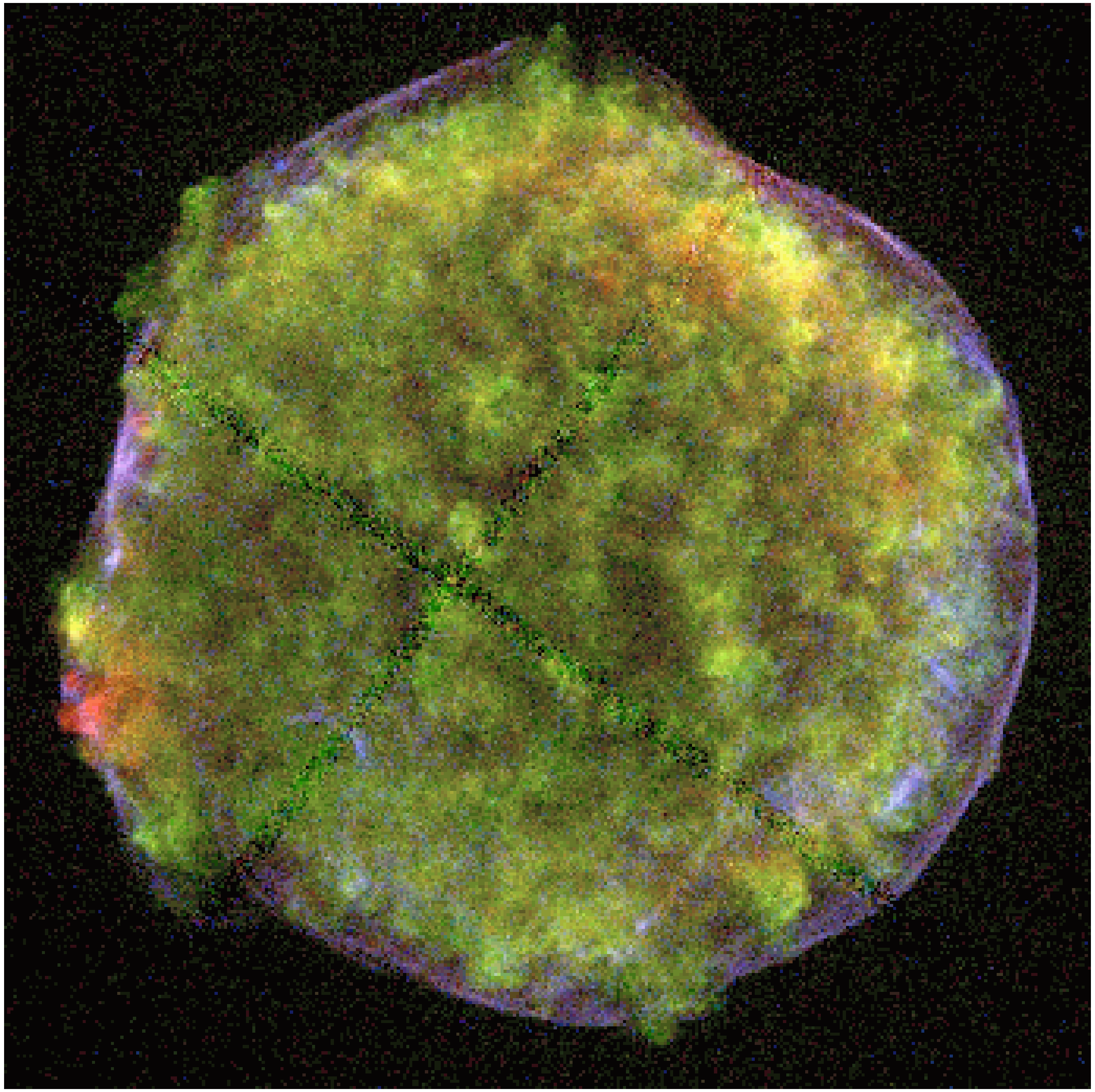

Tycho viewed in X-rays (Warren et al. 2005)

EVIDENCE FOR EFFICIENT DSA IN SNRS

- Thin synchrotron rims:

  The radial profile of the X-ray bright synchrotron rims in Tycho can be explained by models for amplified magnetic fields at the shock front and acceleration of electrons to TeV energies.

  Additionally, the synchrotron dominated rims can be used to constrain the ambient medium density to be 0.6 cm^{-3}.

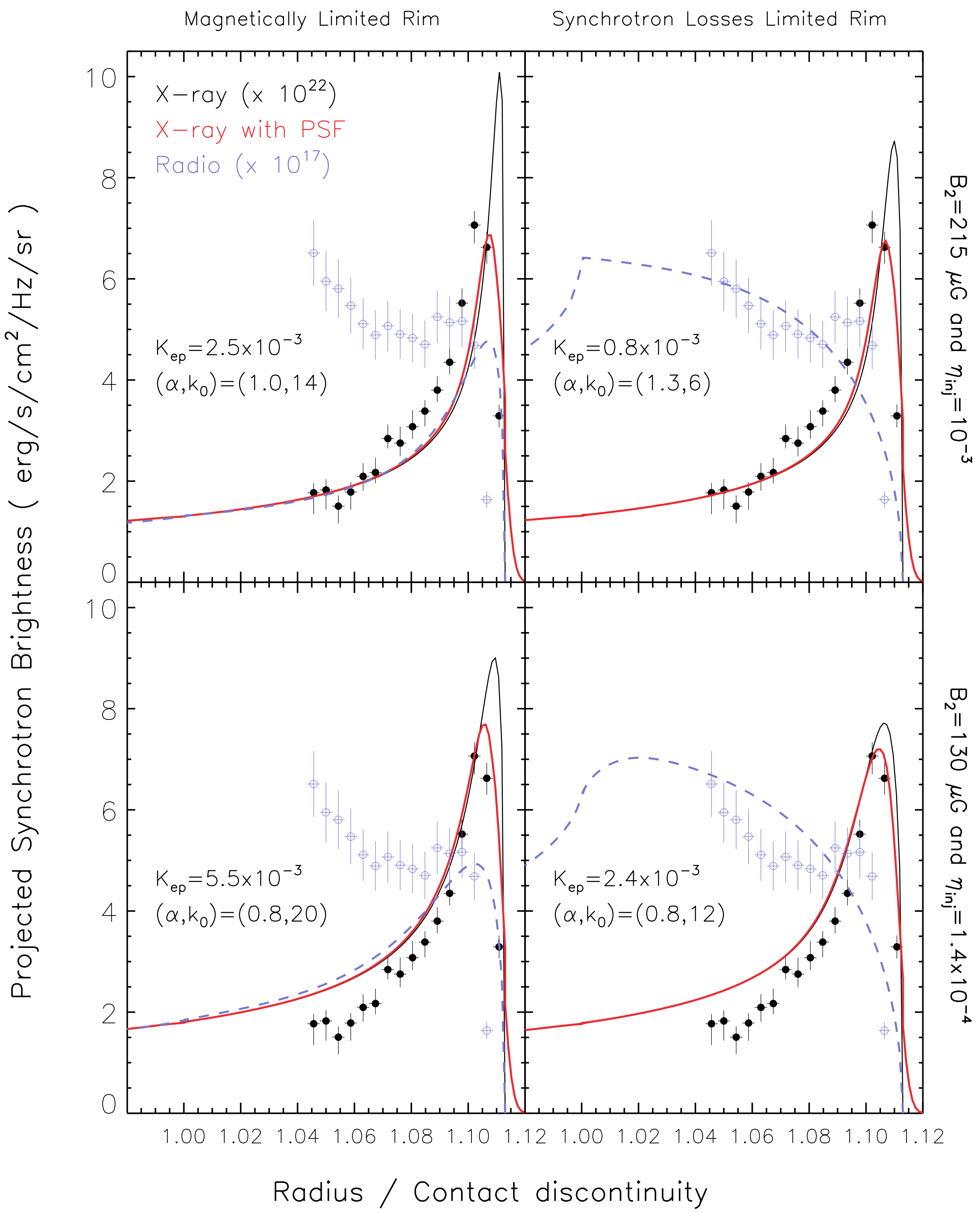

Line of sight projections of radio and X-ray rims with a varying spectral cutoff (α) (Cassam-Chenaï et al. 2007).

Evidence for Efficient DSA in SNRs

TeV γ-ray emission:

HESS detections of TeV gamma rays provides direct evidence for efficient acceleration of particles. However, the origin remains an open question

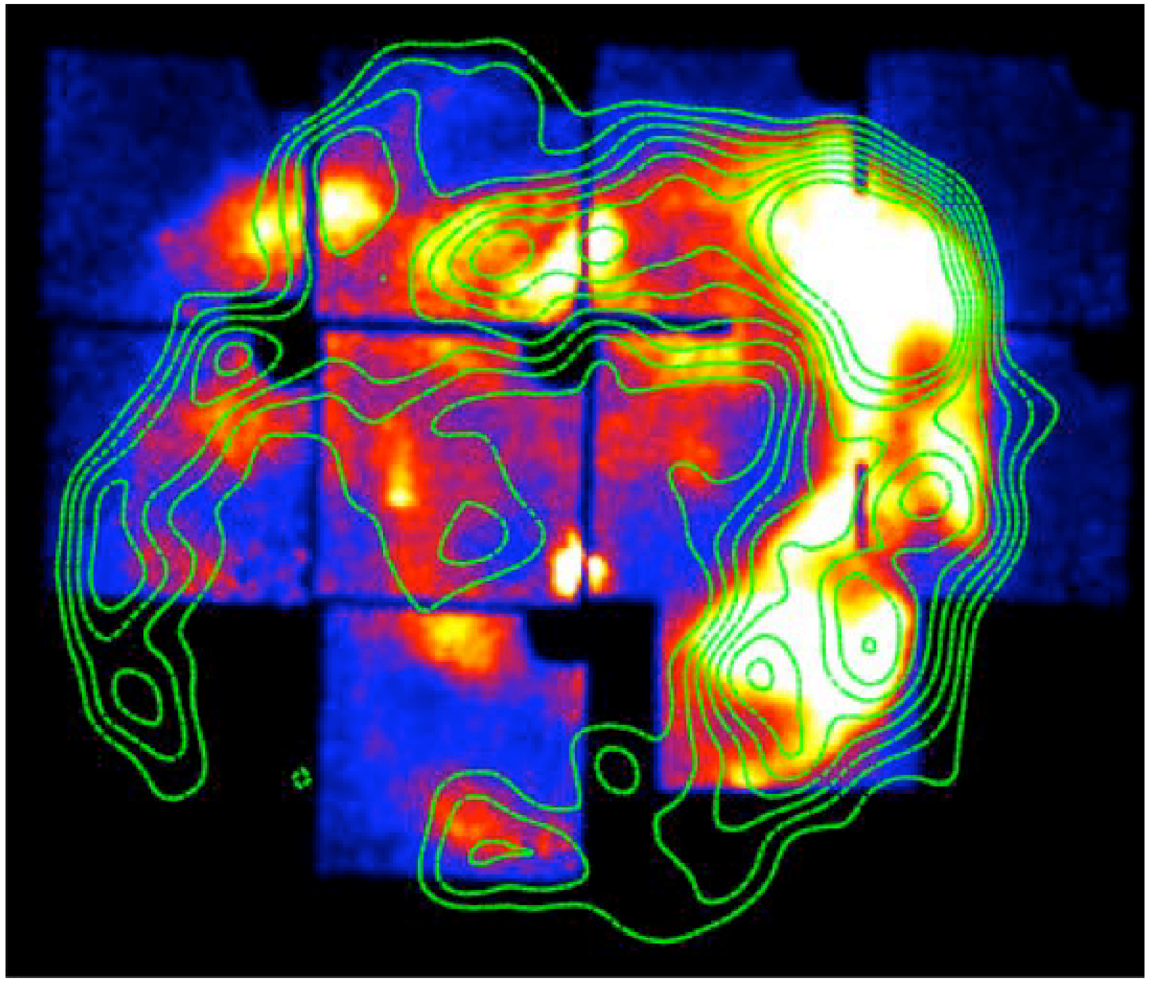

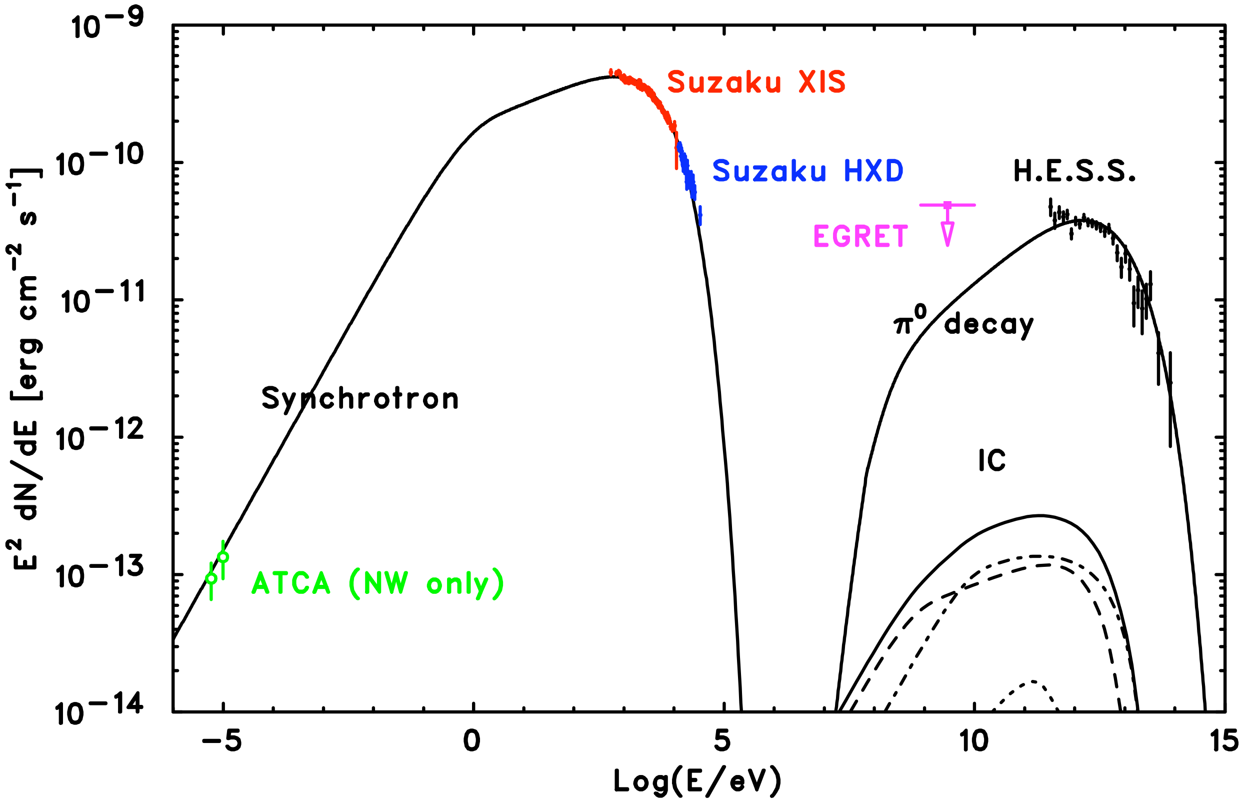

Suzaku XIS image and H.E.S.S. gamma-ray image (contours) of RX J1713-3946. (Left): Broadband SED assuming a hadronic or leptonic origin to the TeV emission (Tanaka et al. 2009).

EVIDENCE FOR EFFICIENT DSA IN SNRS

TeV γ-ray emission:

HESS detections of TeV gamma rays provides direct evidence for efficient acceleration of particles. However, the origin remains an open question

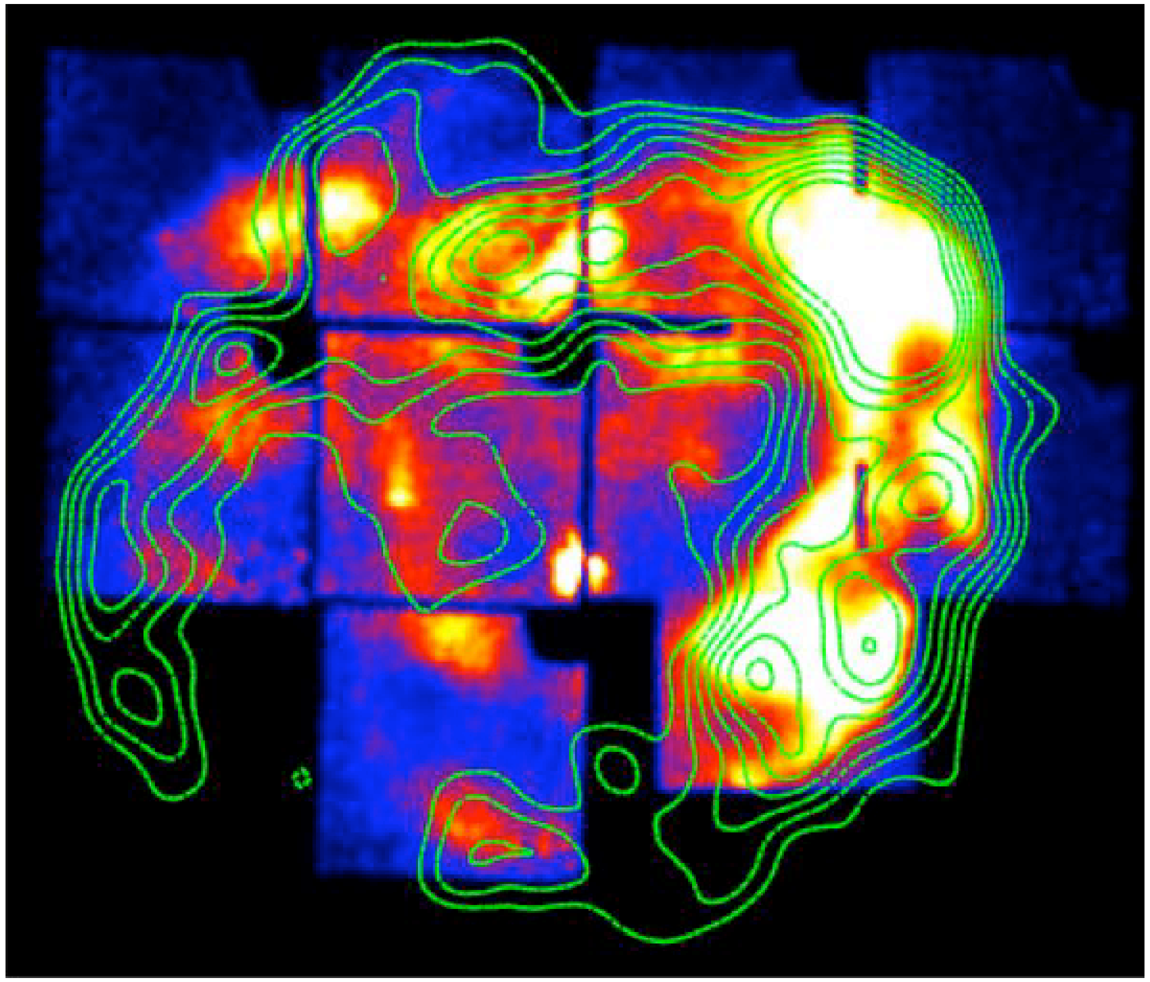

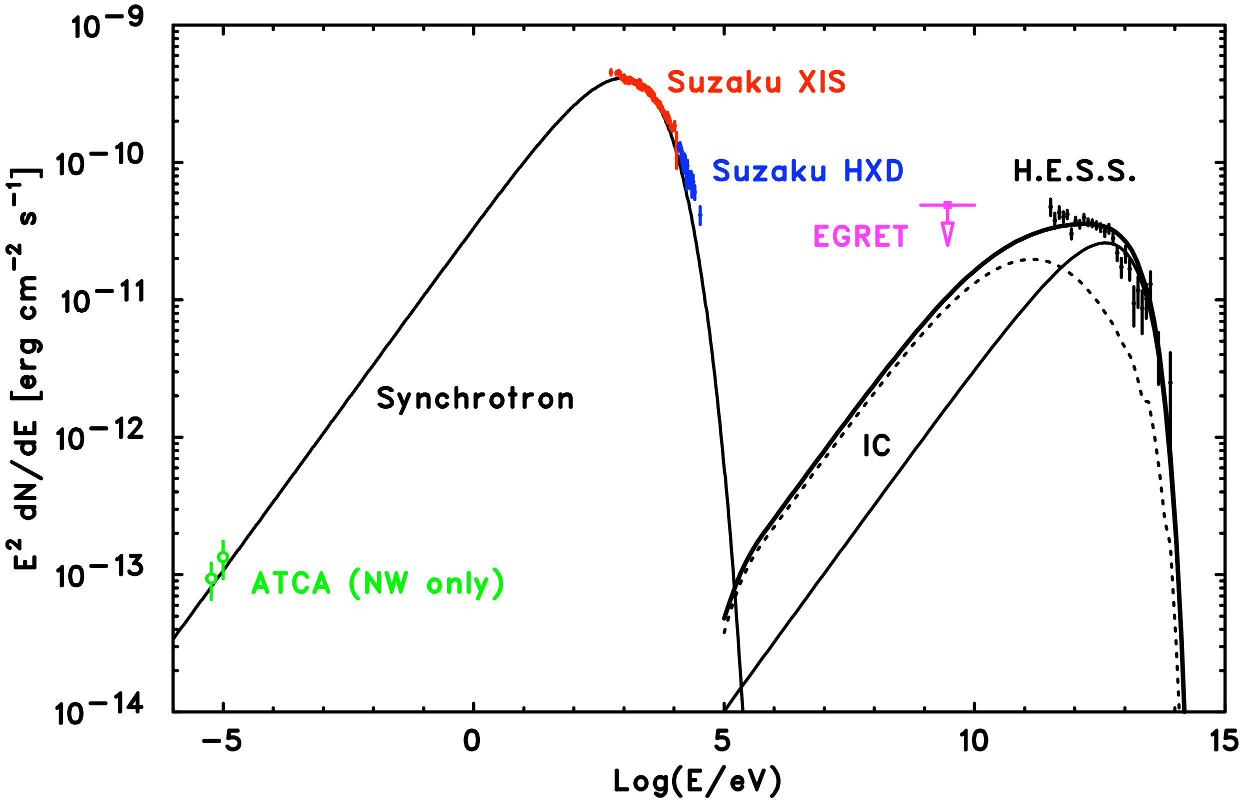

Suzaku XIS image and H.E.S.S. gamma-ray image (contours) of RX J1713-3946. (Left): Broadband SED assuming a hadronic or leptonic origin to the TeV emission (Tanaka et al. 2009).

THE IMPORTANCE OF INCLUDING X-RAY LINE EMISSION IN OUR SIMULATIONS

Often, the lack of thermal emission is used to set the ambient medium density and place constraints upon the source of the TeV emission.

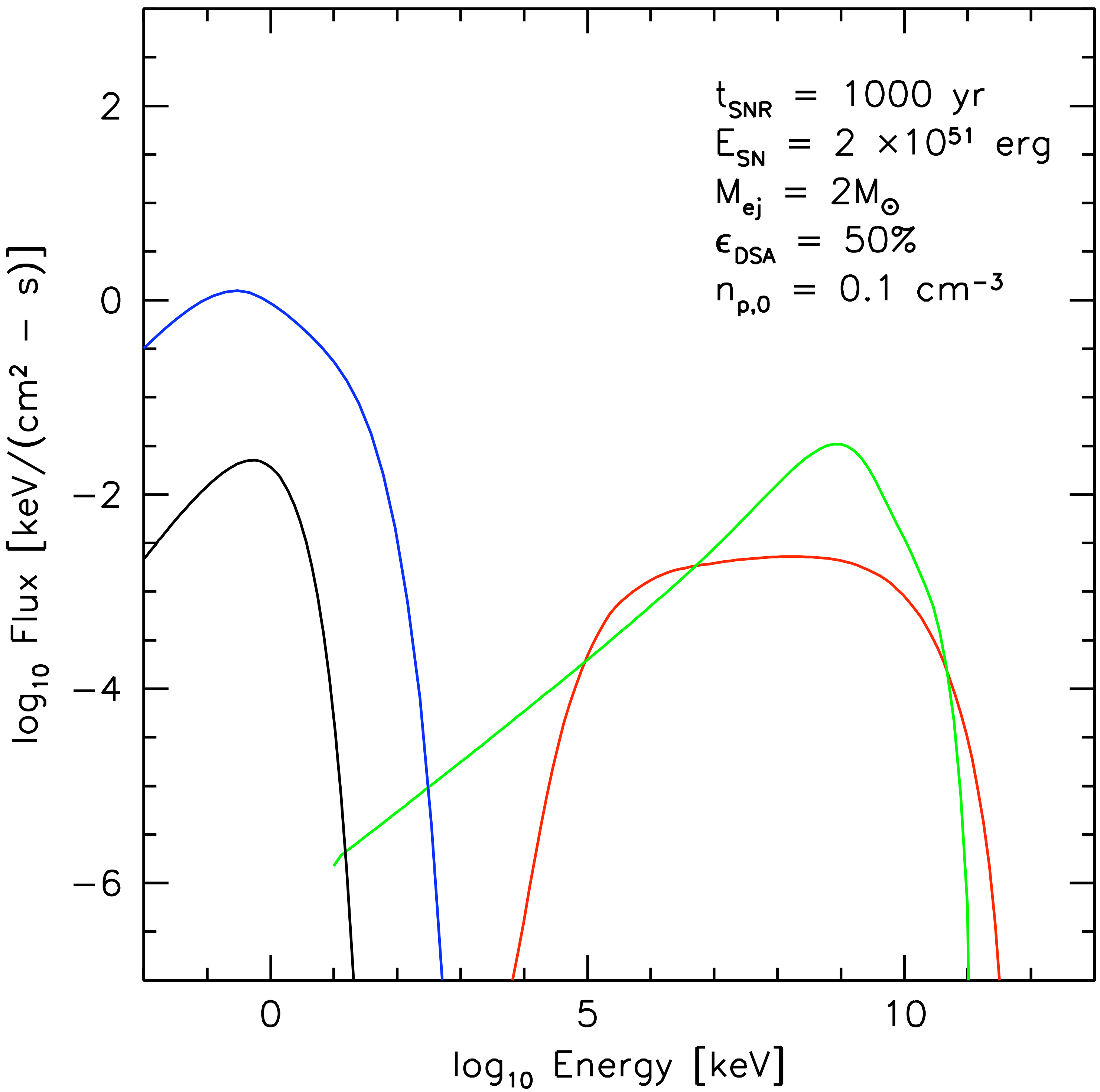

THE IMPORTANCE OF INCLUDING X-RAY LINE EMISSION IN OUR SIMULATIONS

the problem of course is that the X-ray line emission can extend well above the continuum!

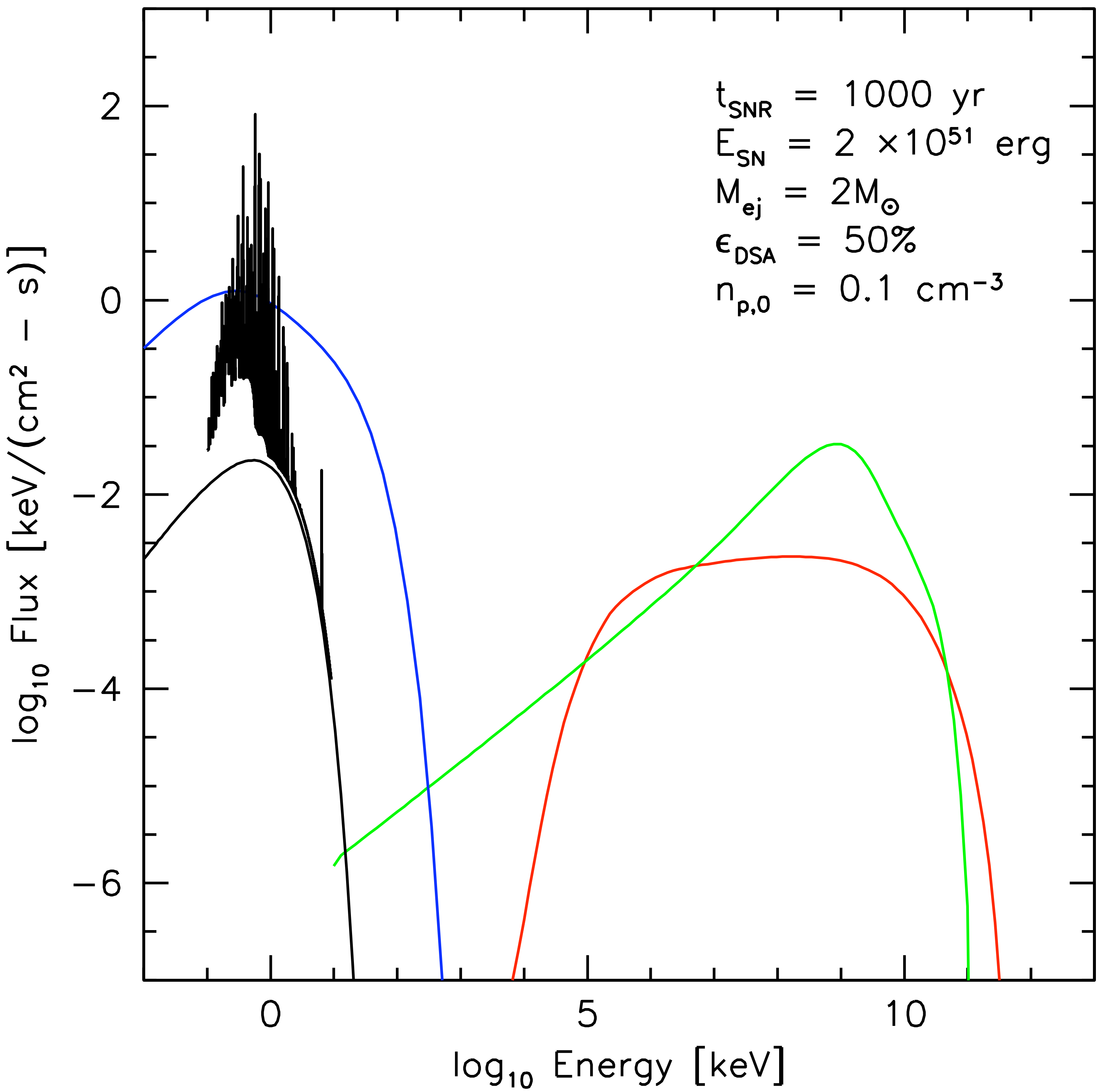

RX J1713-3946:

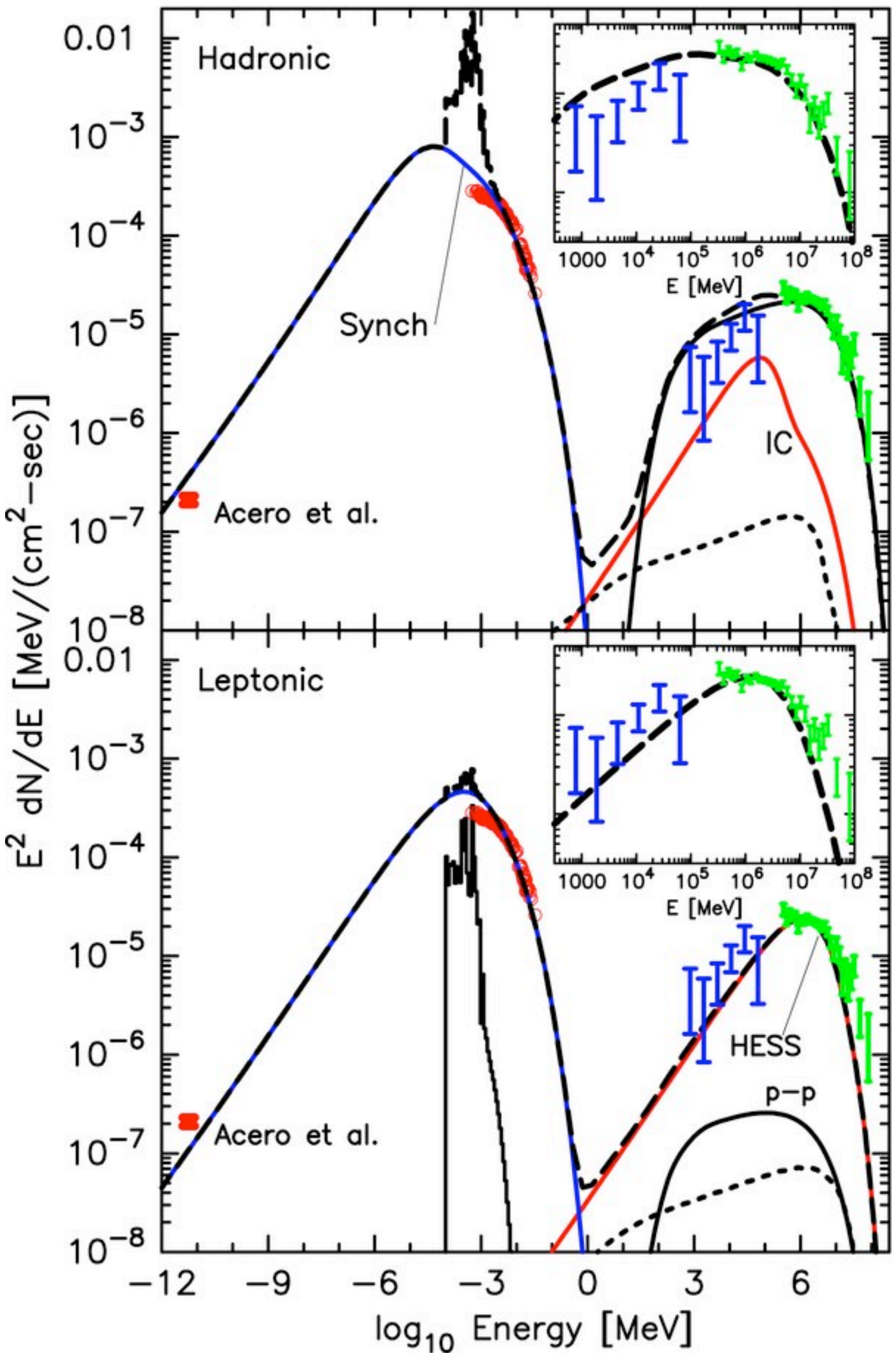

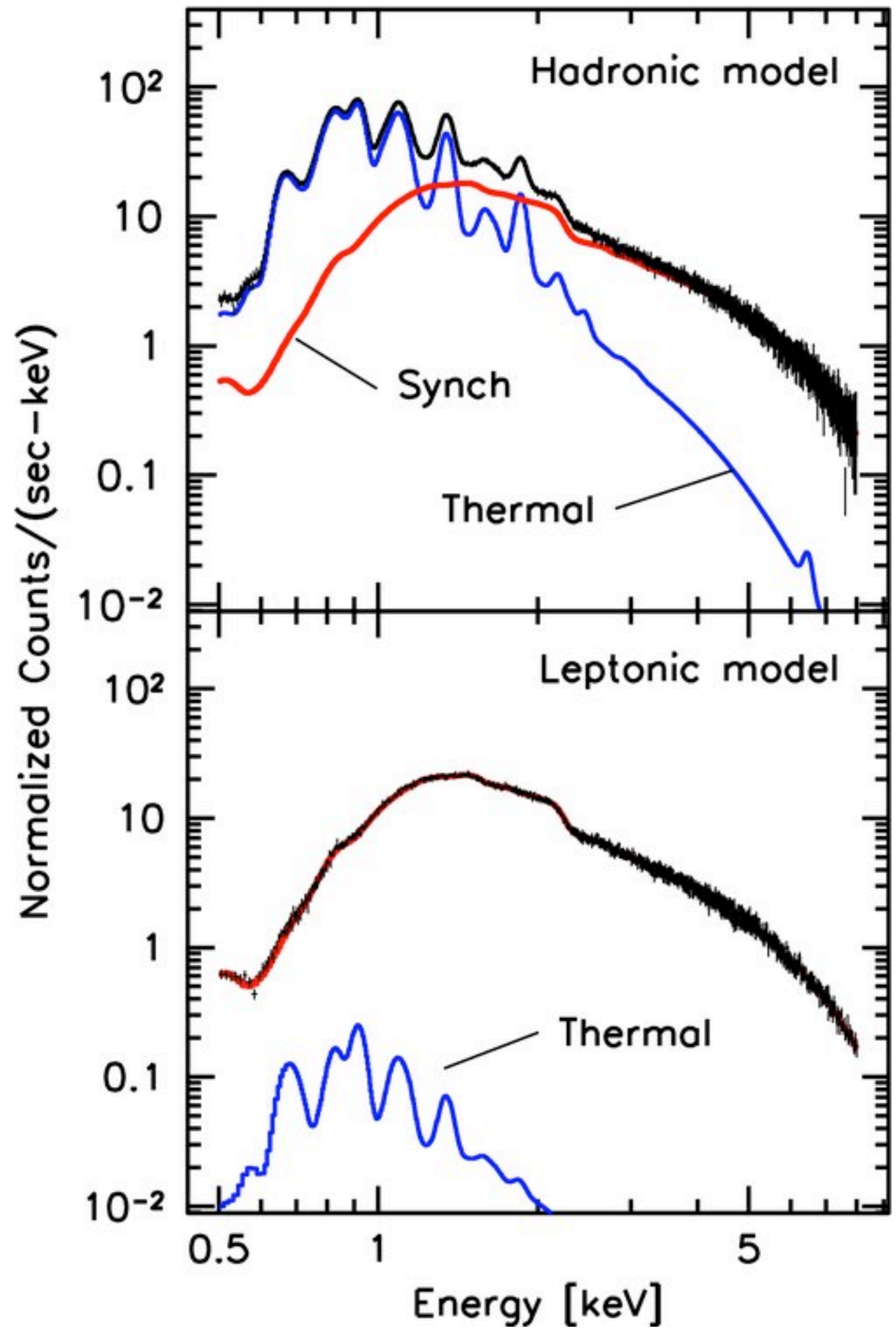

Left: Broadband SED for J1713.
Above: Simulated Suzaku XIS spectrum for J1713 (from Ellison et al. 2010).

Existing evidence suggests that in order to understand the morphology of supernova remnants and other exotic astrophysical objects, we need models that self-consistently calculate the hydrodynamics, diffusive shock acceleration, and nonequilibrium ionization in shocks

OUR MODEL: CR+HYDRO+NEI

- Uses semi-analytic model for DSA of Amato & Blasi (2005) and Blasi (2005)
- The ionization of the shock heated gas at a distance behind the shock is determined by n_e and T_e
- Ionization structure is determined by solving the collisional ionization equations in a Lagrangian gas element
- T_e is calculated by assuming heating via Coulomb collisions, but more efficient heating is considered

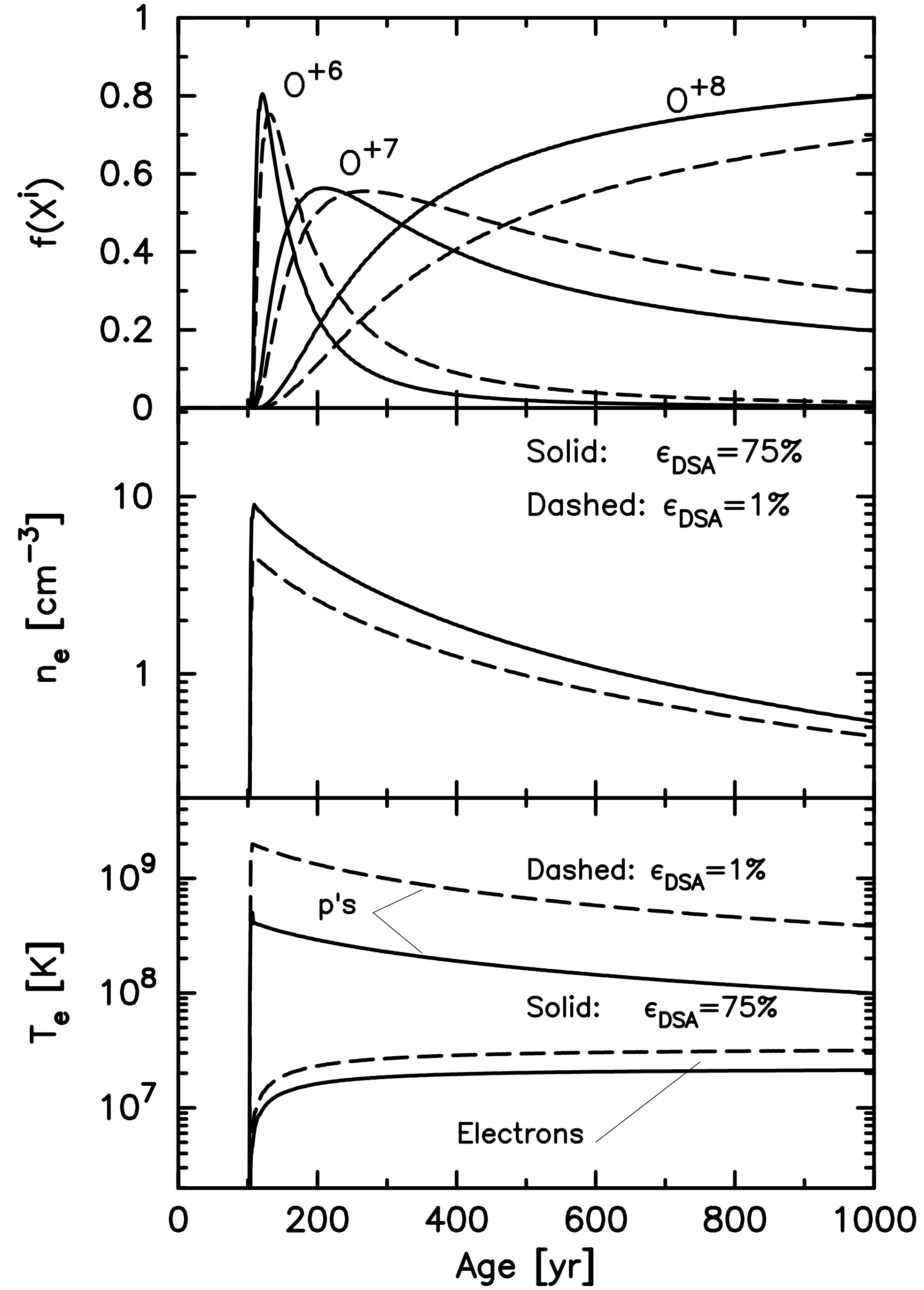

Time evolution of a spherically symmetric Lagrangian mass shell which is crossed by the forward shock at 100 yr. The CSM proton number density for this example is $n_{p,0}$ = 1 cm^{-3}. Here, and in all other examples, the unshocked CSM temperature is T_0 = 10^4 K, and the unshocked magnetic field is B = 15μG.

- Efficient shock acceleration produces a significant nonthermal particle population
- Our model, however, only treats ionization from the thermal population
- Using a Hybrid model (thermal + powerlaw tail) for the electron distribution, Porquet et al (2001) showed that nonthermal effects can alter the ionization balance
- The effect is much less pronounced in ionizing plasmas

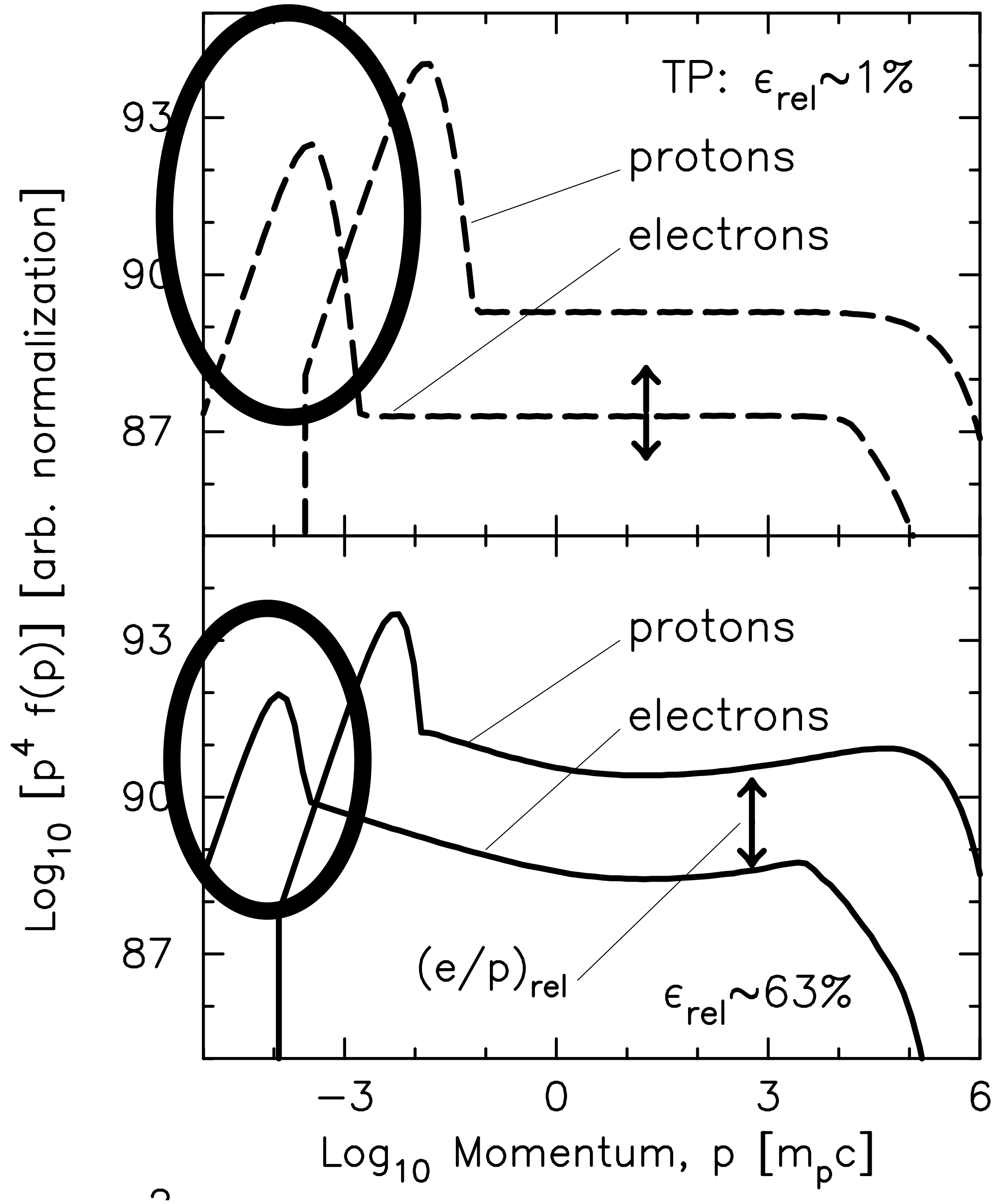

Electron and proton spectra, *$p^4f(p)$,* for TP and efficient DSA. The up/down arrow indicates the normalization of the powerlaw component of the distribution (Ellison et al. 2007).

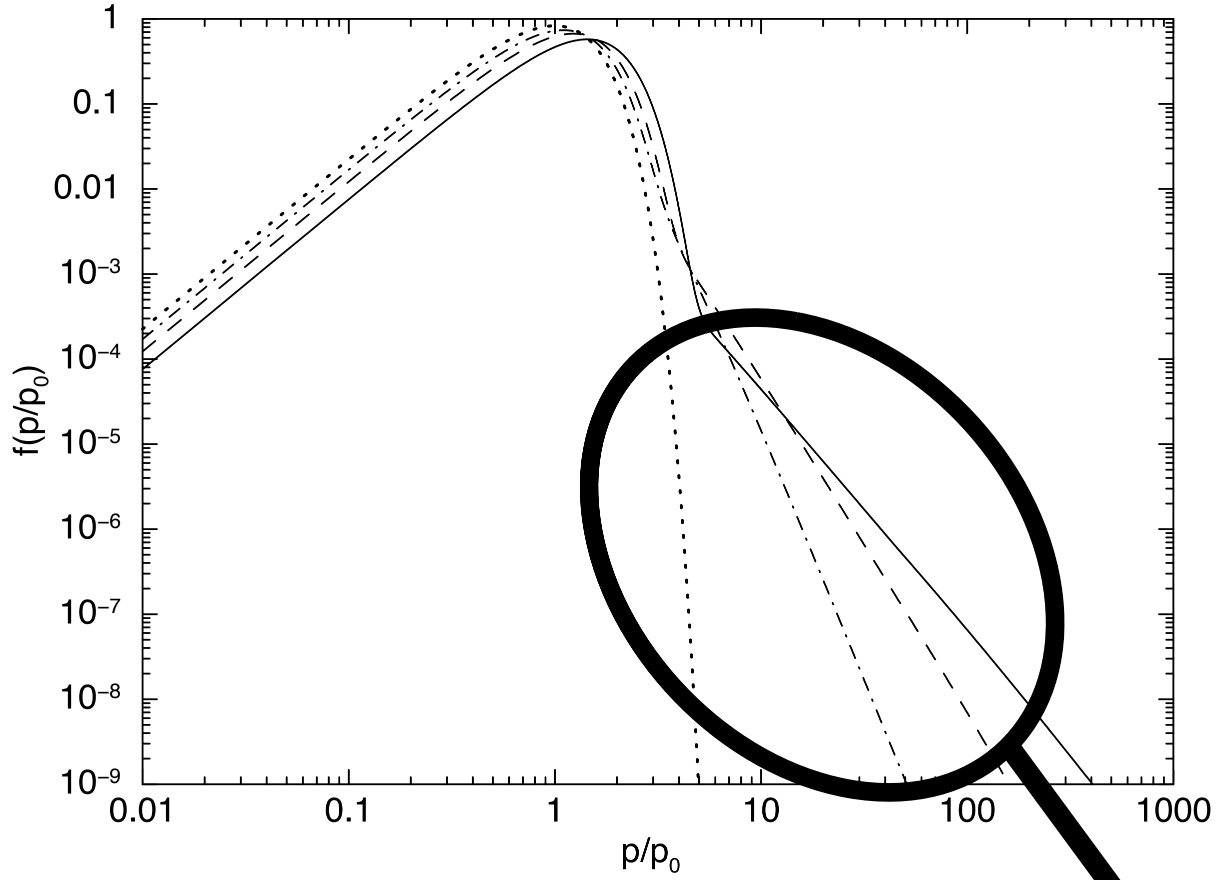

Using a sum of Maxwellians to approximate the particle distribution, Kaastra et al. (2009) showed that the prescence of nonthermal particles can alter the relative intensities of satellite lines.

Above: summed particle distribution function behind a cluster shock. Right: simulated IXO spectrum (crosses) with the best fit Maxwellian-plasma model, showing an excess at Fe XXV j line.

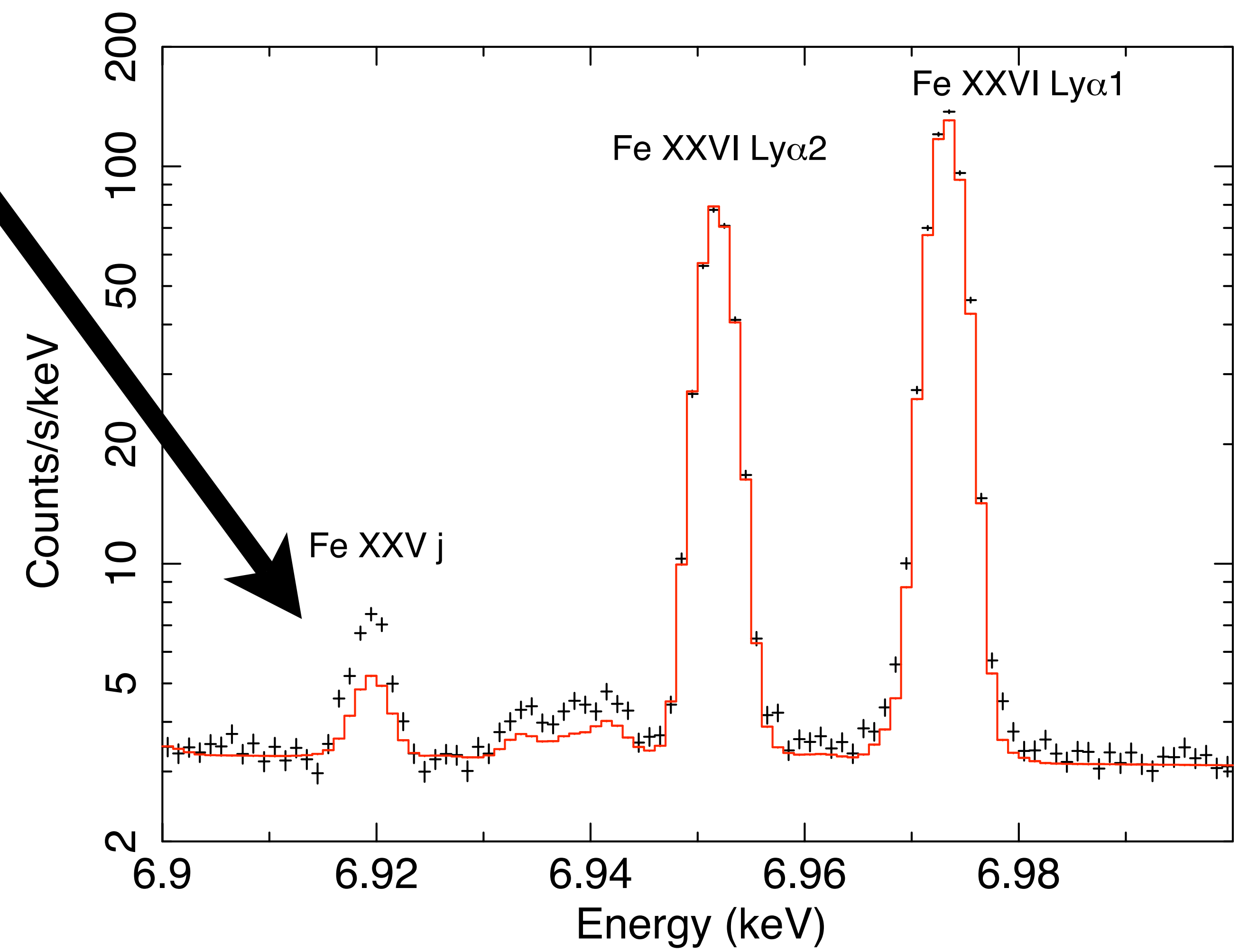

EXAMPLE RESULTS:

- In the efficient models, the charge state for a particular ion peaks closer to the shock front
  - For instance, in the $n_{p,0}$ = 1.0 cm^{-3} models, O^{6+} ~ 2″ behind the FS for efficient models, and ~ 4″ behind for test particle models
- The resolved spatial and spectral structure could provide useful diagnostics for Galactic SNRs undergoing efficient shock acceleration

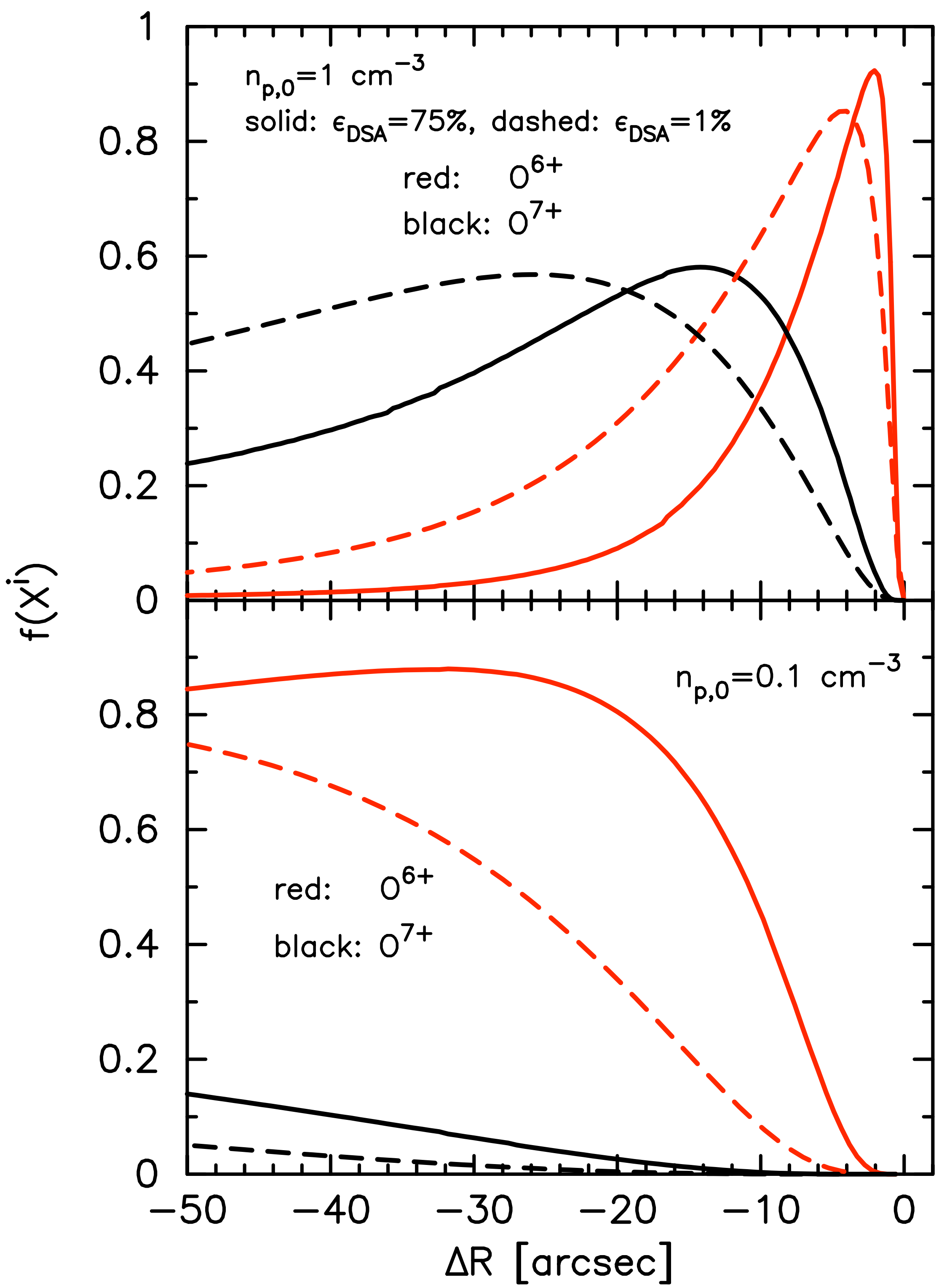

Top: Ionization fraction as a function of distance behind the forward shock for O^{6+} and O^{7+} with $n_{p,0}$ = 1.0 cm^{-3}. Bottom: Ionization fractions of O^{6+} and O^{7+} with $n_{p,0}$ = 0.1 cm^{-3}. In both panels, the solid curves are for ϵ_{DSA} = 75% and the dashed curves are for ϵ_{DSA} = 1%. The angular scale is determined assuming the SNR is at a distance of 1 kpc and the results are calculated at t_{SNR} = 1000 yr.

IONIZATION AGE VS ACCELERATION EFFICIENCY:

- Simulation also tracks ionization age ($n_e t$)
- For increasing acceleration efficiency, SNRs appear to have a higher ionization age
- Additionally, models with higher E_{sn} but lower acceleration efficiency can appear spectrally similar to models with lower E_{sn} but differing acceleration efficiencies

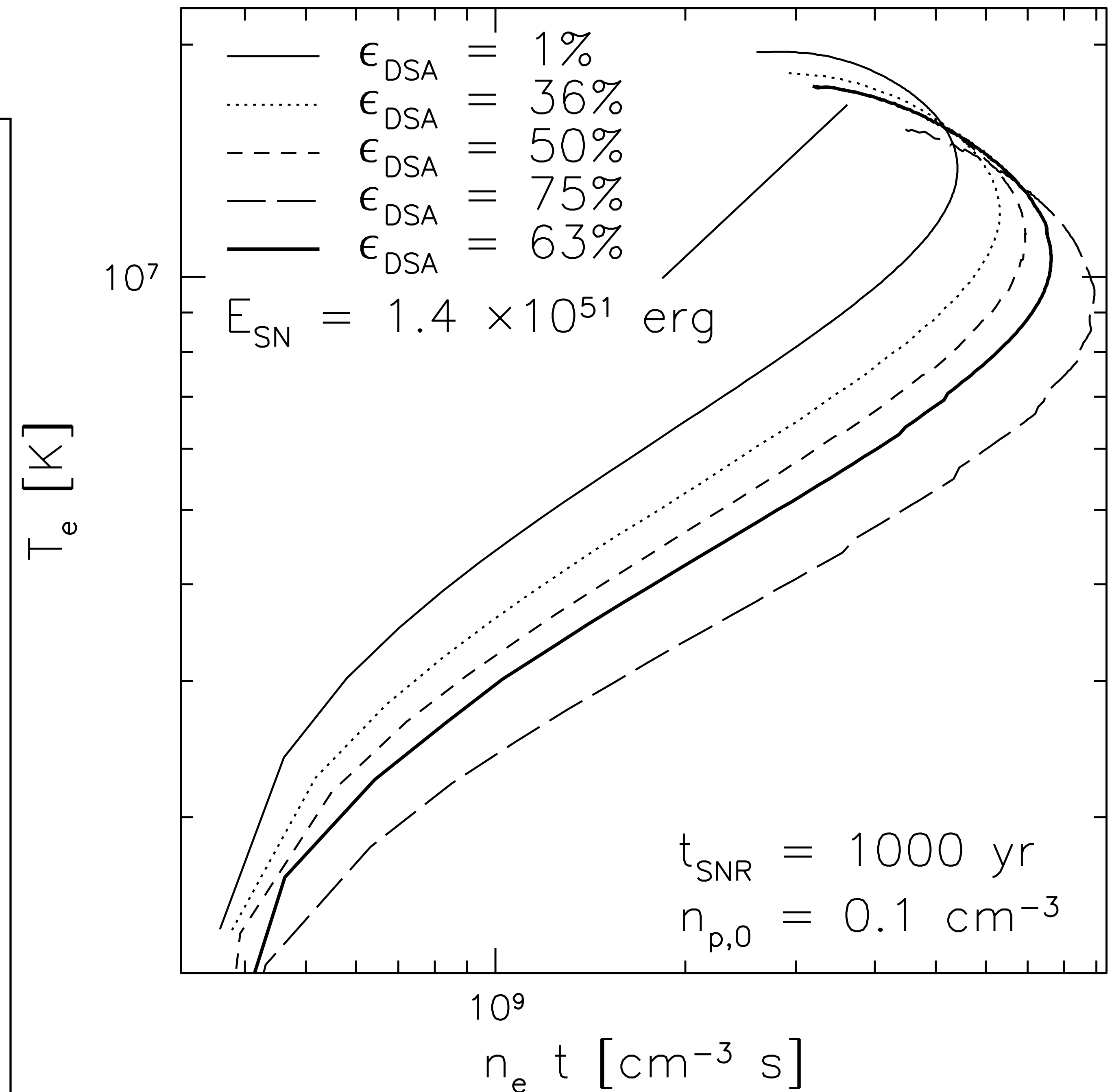

$n_e t$ vs T_e for varying acceleration efficiency. In these curves, the forward shock is in the lower left, and the contact discontinuity is at the upper right.

THERMAL X-RAY EMISSION

Specify:

E_{sn}, M_{ej}, n_{amb}, ε_{DSA},...

→

Calculate:

NEI, hydro, DSA, etc

→

Observables:

SNR dynamics, emitted spectrum

EXAMPLE RESULTS:

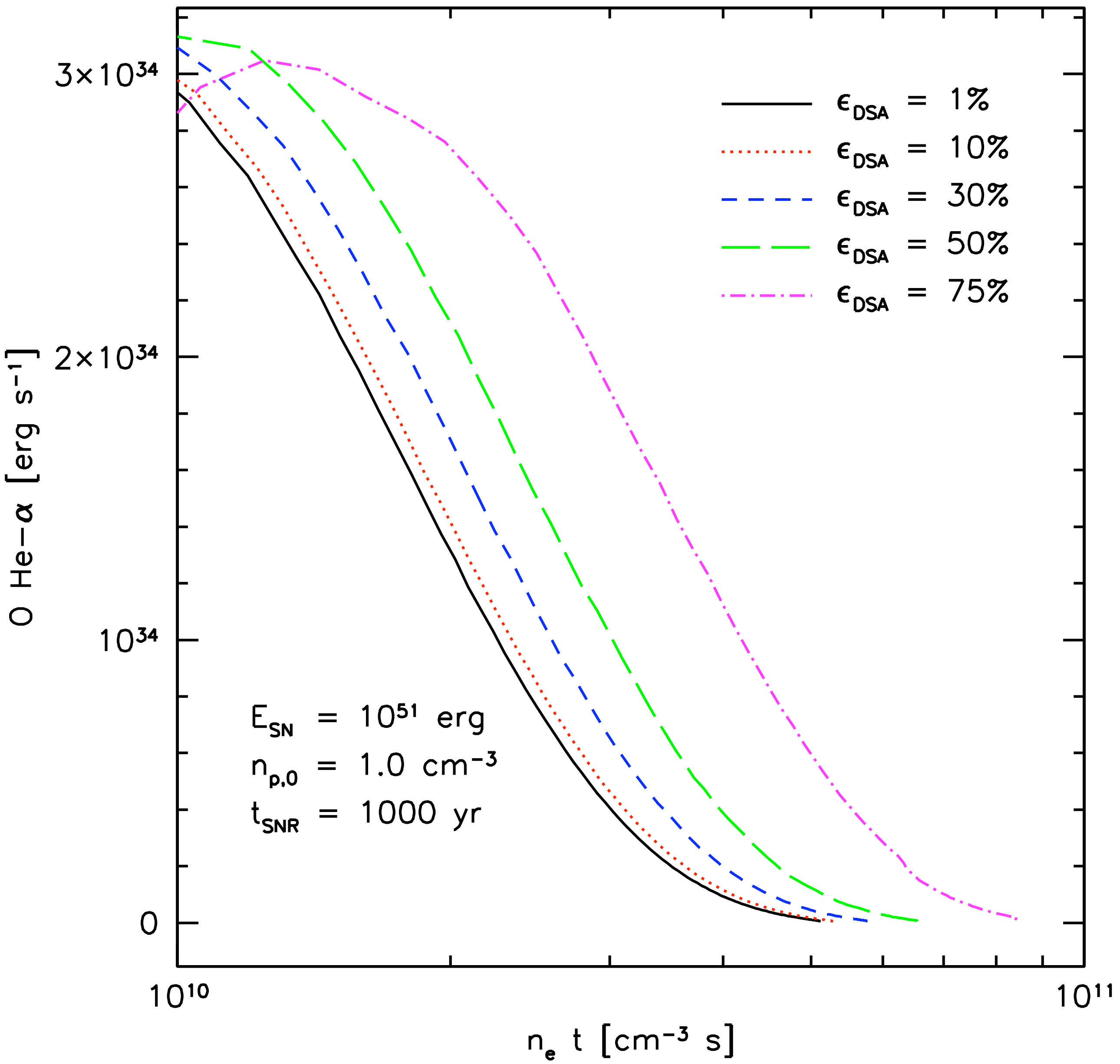

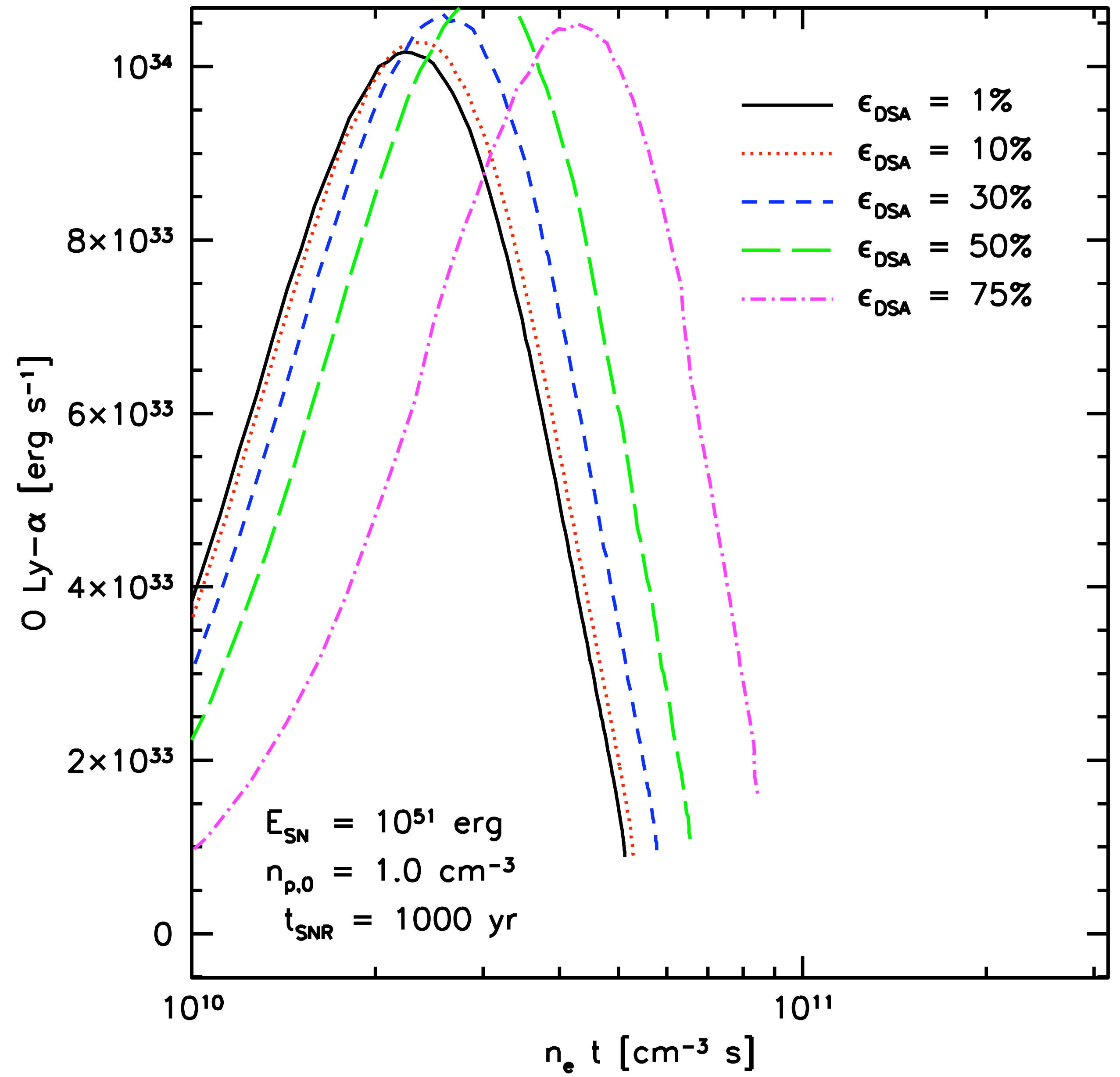

Left: He-like O emission vs τ for varying ε_{DSA}. Right: Same, but for H-like O. Both plots show higher ionization ages at the same SNR age.

EXAMPLE RESULTS:

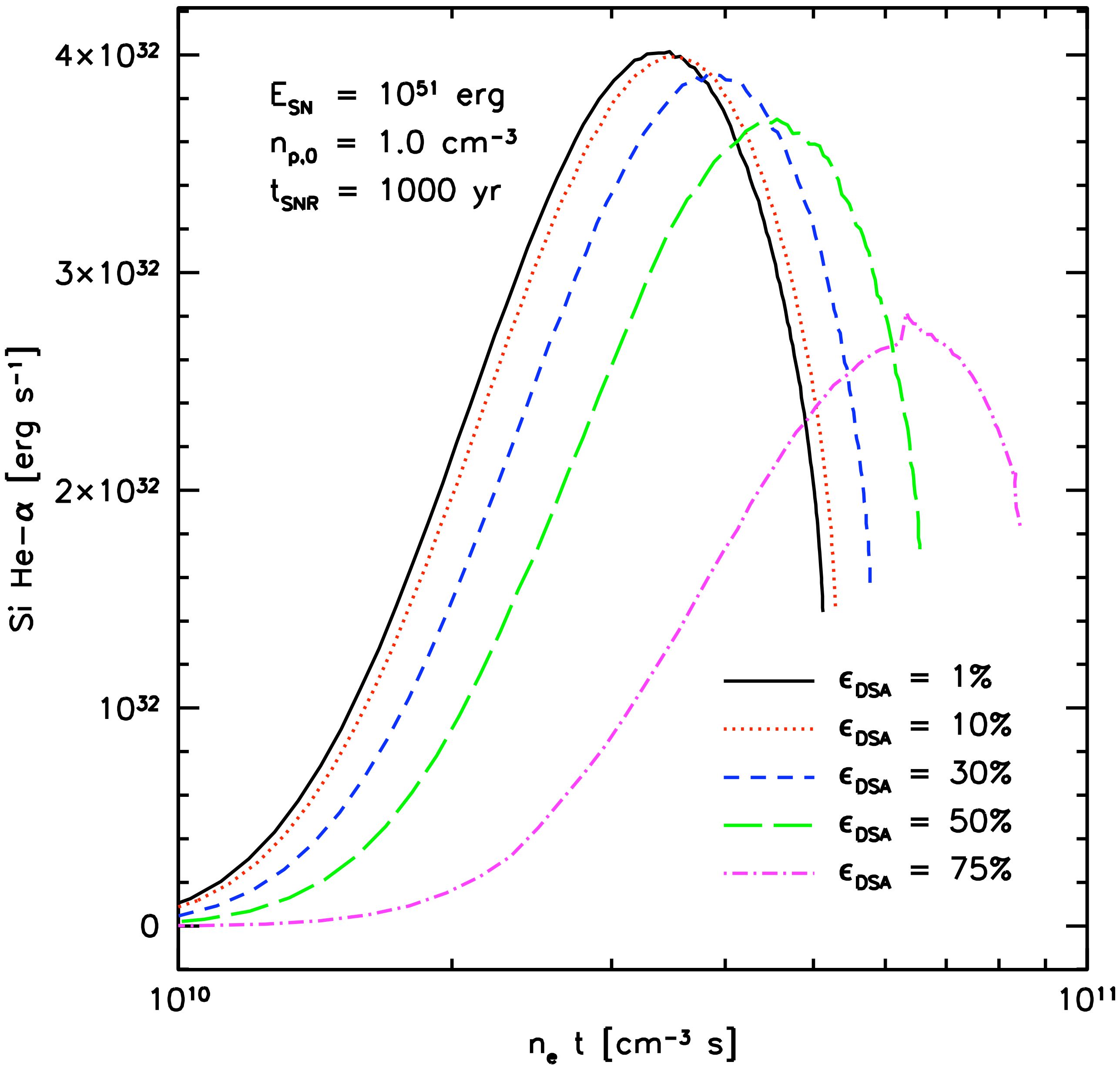

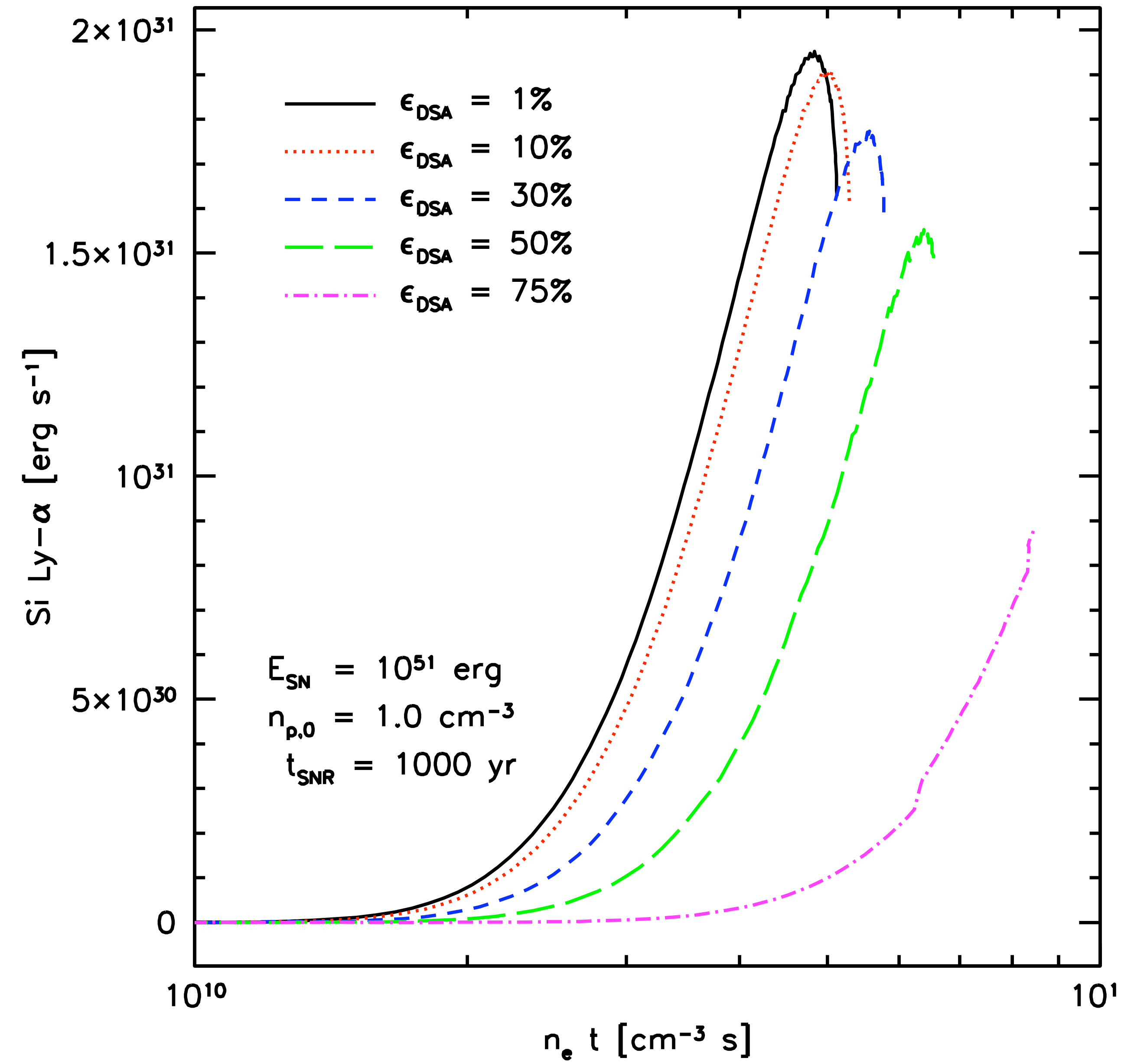

Left: He-like Si emission vs τ for varying ε_{DSA}. Right: Same, but for H-like Si. Both plots show higher ionization ages at the same SNR age.

Fast Variability in Nonthermal Emission Filaments in SNRs

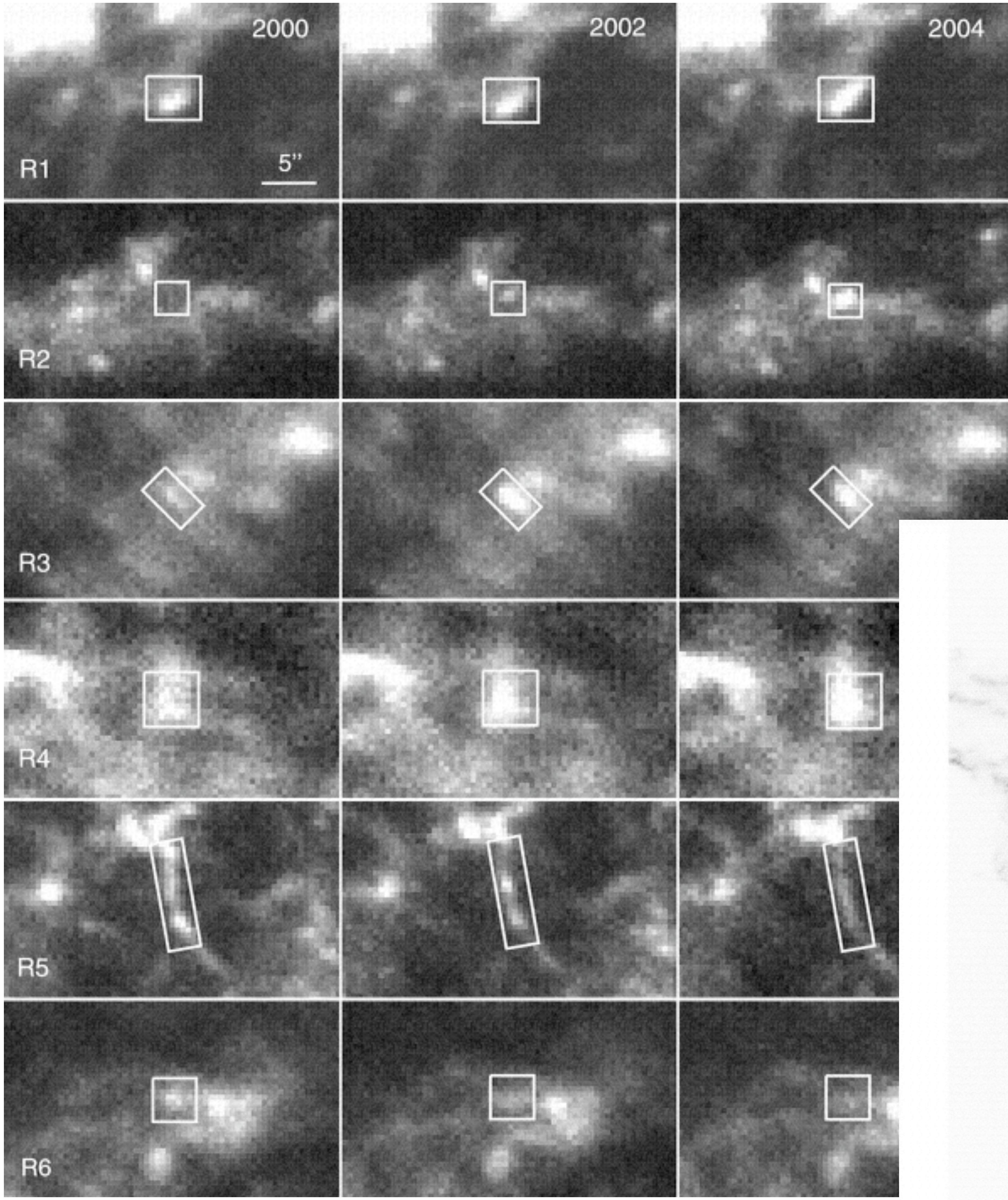

Multi-epoch images of Cas A show changes in the thermal and nonthermal emission from small, ~ 0.03 pc (Patnaude & Fesen 2007)

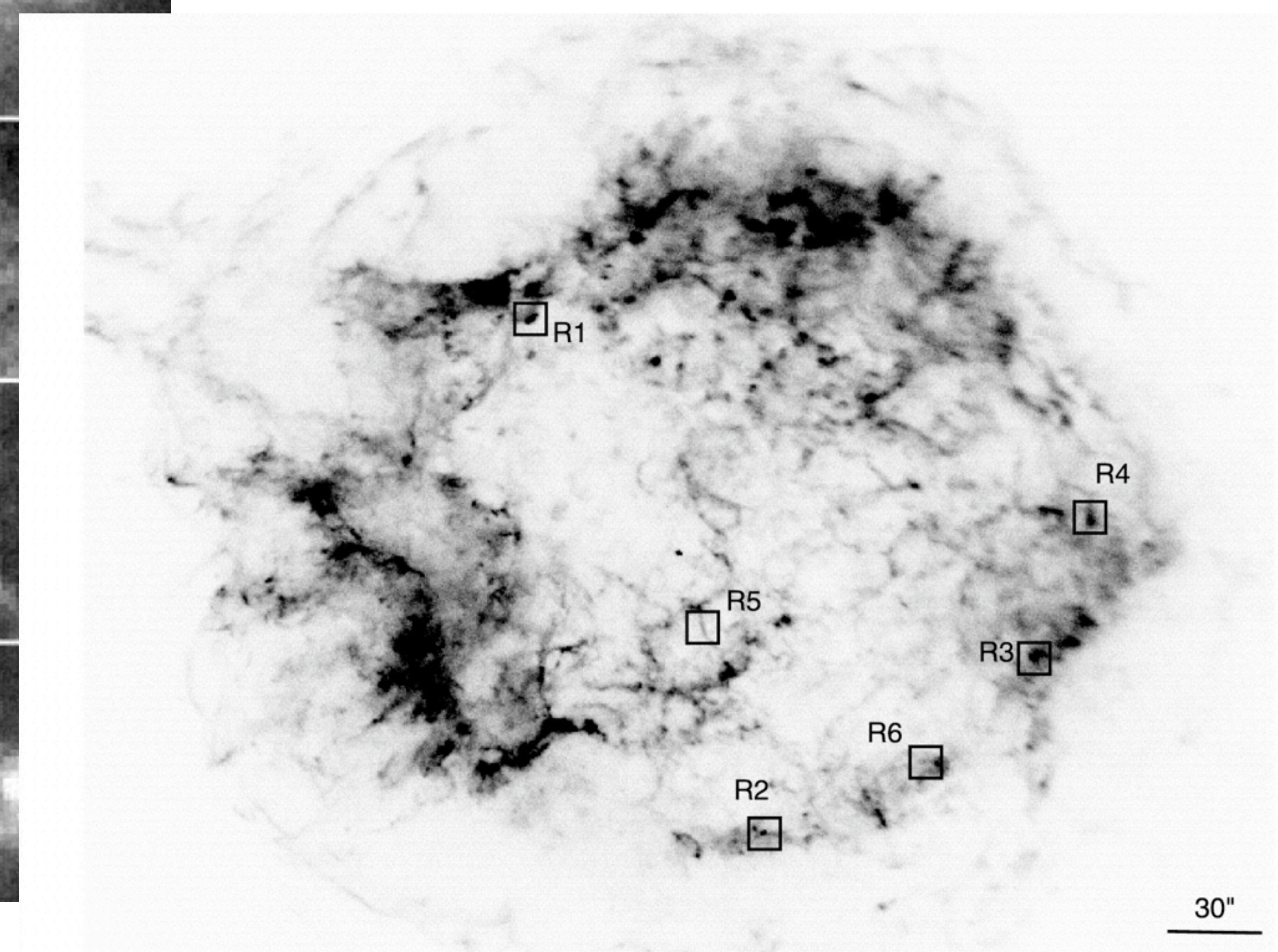

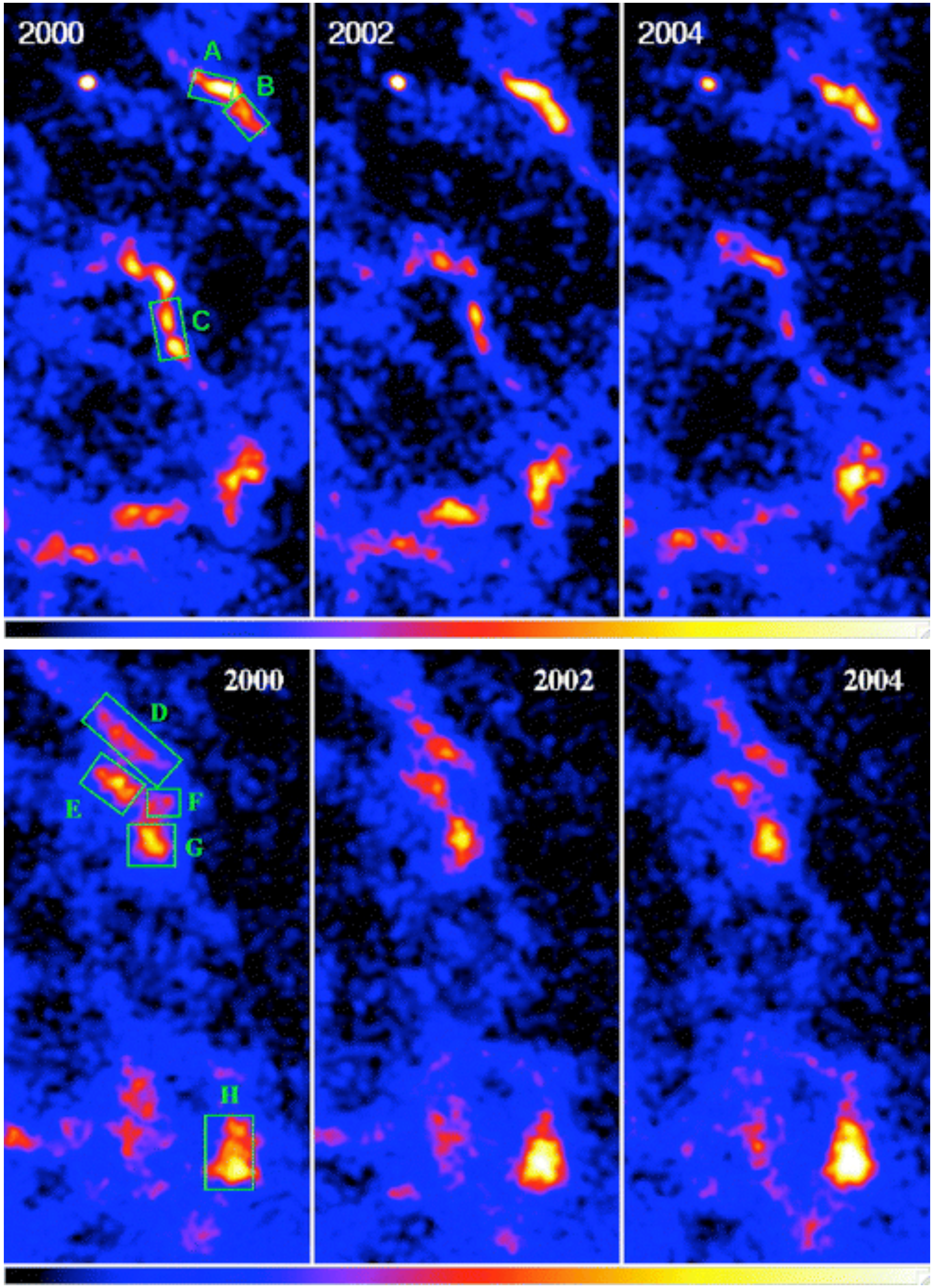

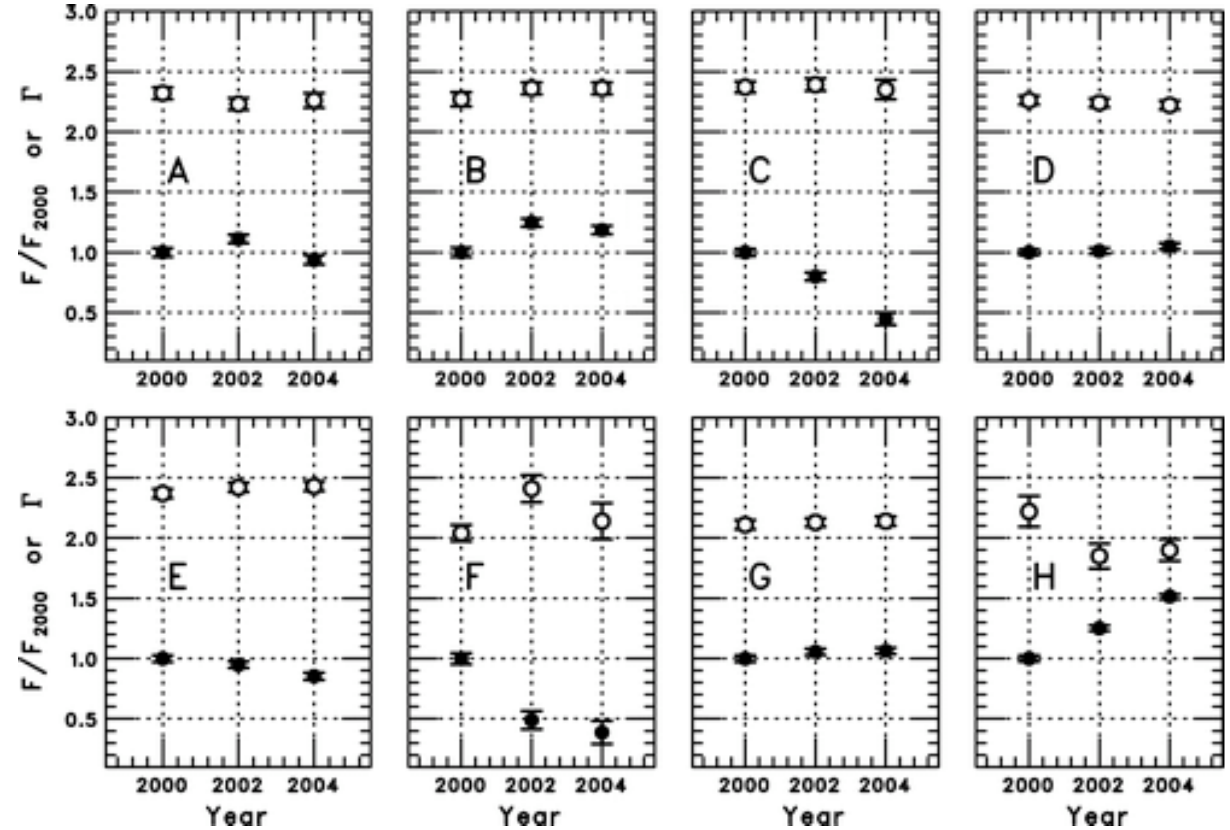

$$\Gamma \approx \text{constant}$$

$$\rightarrow B \approx \text{constant}$$

Uchiyama & Aharonian (2008) interpreted the changes in nonthermal emission filaments as evidence for efficient acceleration at the SNR reverse shock.

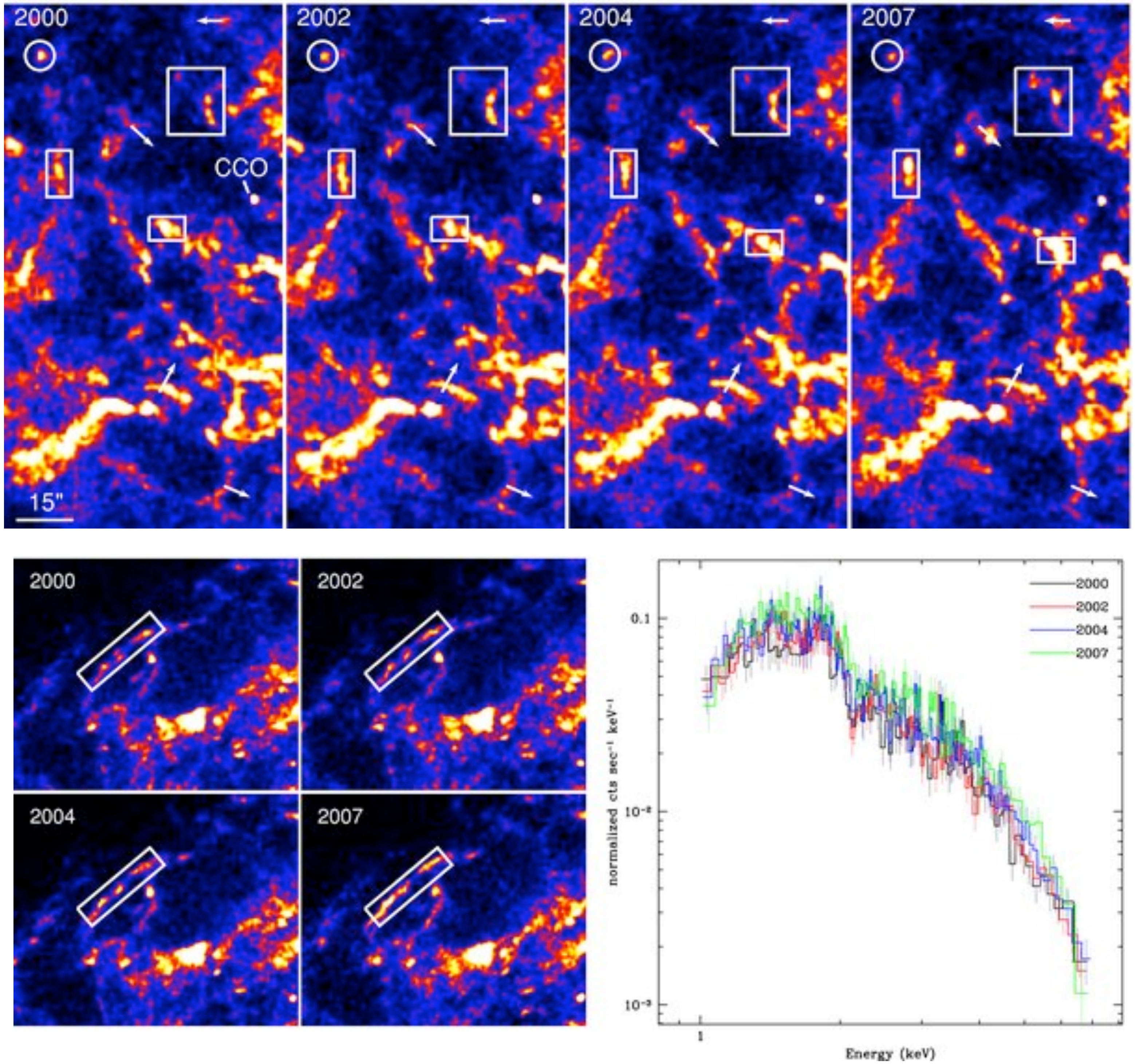

Top: Interior filaments of Cas A showing changes in brightness and position of nonthermal filaments. Bottom: Northeast filament and spectrum. The spectrum is not changing, except for intensity.

Changes seen in 2000-2004 observations are seen in 2007 as well (Patnaude & Fesen 2009)

Nonthermal emission filaments show apparent random and nonradial motions

Filaments in the interior (top panels) show similar changes in brightness as filaments that are shown in “external” filaments

What is the origin of the changes seen in the emission?

Bykov et al. (2008) interpreted the flickering in the context of Alvén waves in a turbulent postshock magnetic field

The observed spatial scales in their simulations are ~ 10^{16} cm

Timescales for variations in flux from 1 keV photons are ~ 1 year

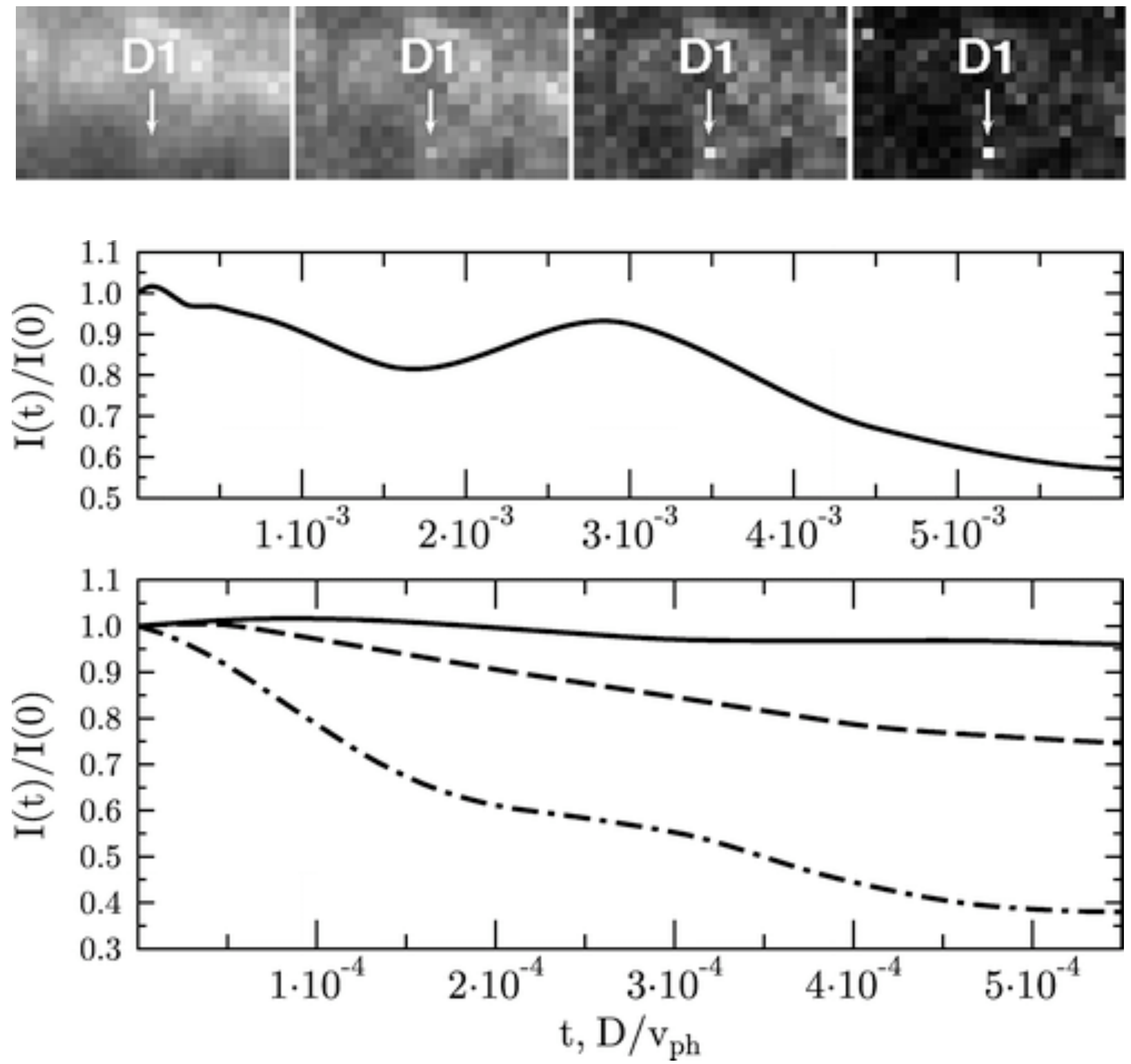

Top: Emissivity of a shocked clump vs energy. Bottom: Light curve for clump D1.

New 2009 Observations:

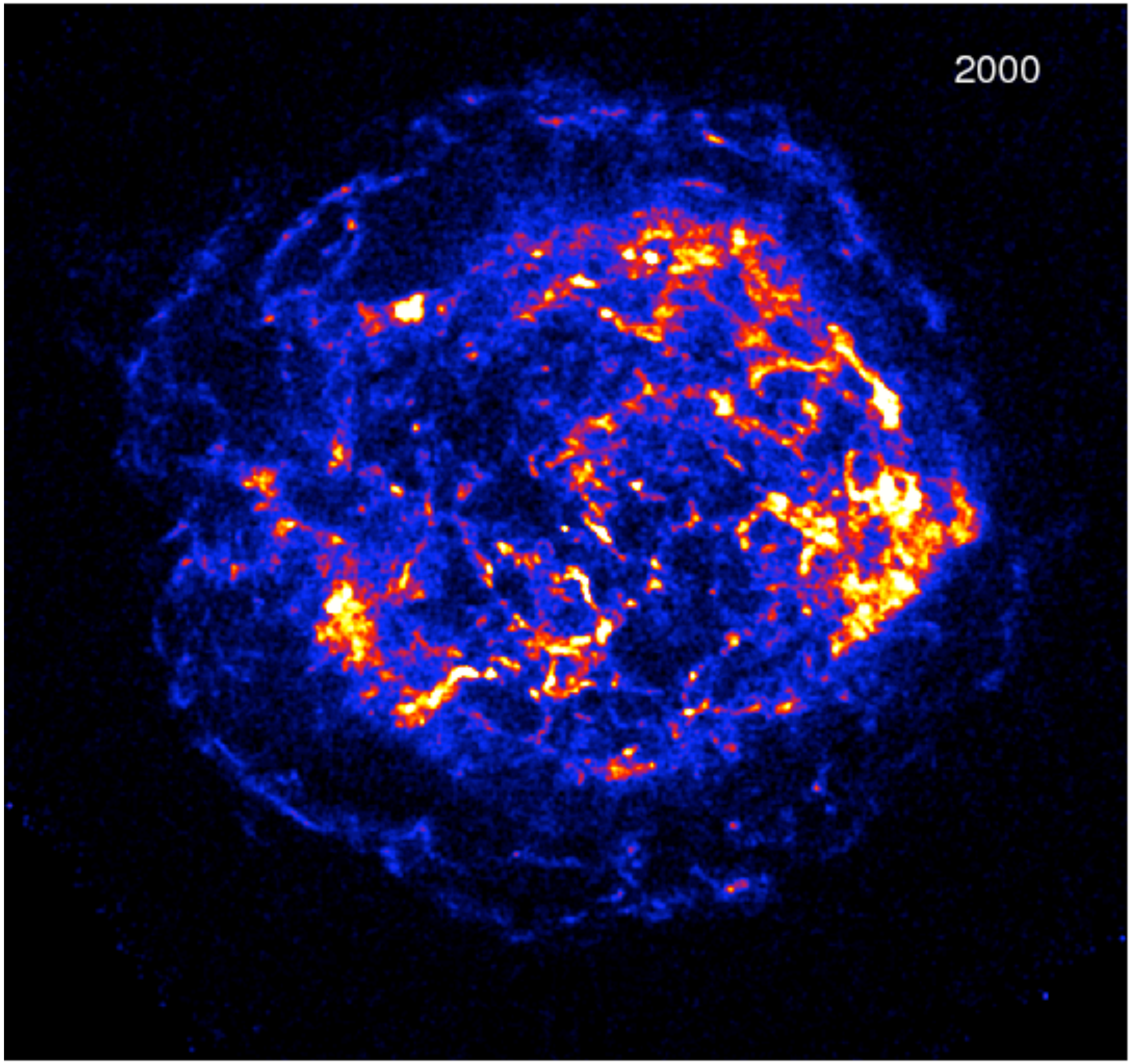

$$
\begin{aligned}
\text{for } B &\sim \text{const} \\
\frac{\delta J_\nu}{J_\nu} &\sim \frac{\delta n}{n} \\
v_{\rm sh} &= 5 \times 10^8 \text{ cm s}^{-1} \\
t_{\rm loss} &= 2 \text{ yr} \\
\delta x &\sim v_{\rm sh} \times \; t_{\rm loss} \\
&\sim 0.01 \text{ pc} \\
&\sim \delta x_{\rm QSF} \\
\delta J_\nu &\sim \delta x_{\rm QSF}
\end{aligned}
$$